EFDA–JET–PR(11)37

T. Zhang, Y. Liang, S. Soldatov, A. Fonseca, Y. Xu, K. Crombe, L. Frassinetti, M.N.A. Beurskens, Y. Sun, B. Alper, E.R. Solano, P.J. Lomas, H.R. Koslowski, J. Pearson, Y. Yang and JET EFDA contributors

Influence of Resonant Magnetic Perturbation (RMP) on the Turbulence in the Edge Pedestal on JET

Influence of Resonant Magnetic Perturbation (RMP) on the Turbulence in the Edge Pedestal on JET

T. Zhang[1], Y. Liang[1], S. Soldatov[1,2], A. Fonseca[3], Y. Xu[4], K. Crombé[2], L. Frassinetti[5], M.N.A. Beurskens[6], Y. Sun[1], B. Alper[6], E.R. Solano[7], P.J. Lomas[6], H.R. Koslowski[1], J. Pearson[1], Y. Yang[1,8] and JET EFDA contributors*

JET-EFDA, Culham Science Centre, OX14 3DB, Abingdon, UK

[1]Forchungszentrum Jülich, Institute of Energy and Climate Research -Plasma Physics, EURATOM Association, D-52425, Jülich, Germany
[2]Department of Applied Physics UG (Ghent University) Rozier 44 B-9000 Ghent Belgium
[3]Associação EURATOM/IST, Instituto de Plasmas e Fus~ao Nuclear, Instituto Superior Tecnico, Av Rovisco Pais, 1049-001 Lisbon, Portugal
[4]Association "EURATOM-Belgian state" Laboratory for Plasma Physics Koninklijke Militaire School-Ecole, Royal Militaire Renaissancelaan 30 Avenue de la Renaissance B-1000 Brussels Belgium
[5]Division of Fusion Plasma Physics, School of Electrical Engineering, Royal Institute of Technology, Association EURATOM-VR, Stockholm, Sweden
[6]EURATOM-CCFE Fusion Association, Culham Science Centre, OX14 3DB, Abingdon, OXON, UK
[7]Laboratorio Nacional de Fusion, Asociacion EURATOM-CIEMAT, 28040, Madrid, Spain
[8]Institute of Plasma Physics, Chinese Academy of Sciences, PO Box 1126, Hefei, Anhui 230031, People's Republic of China
** See annex of F. Romanelli et al, "Overview of JET Results", (23rd IAEA Fusion Energy Conference, Daejon, Republic of Korea (2010)).*

Preprint of Paper to be submitted for publication in
Plasma Physics and Controlled Fusion

ABSTRACT.
The influence of an n = 2 Resonant Magnetic Perturbation (RMP) field on the density fluctuation in the edge pedestal has been investigated using correlation reflectometry in type-I ELMy H-mode plasma on JET. Without the n = 2 field, the frequency spectrum of the density fluctuation shows two broadband fluctuation components: one is with Low Frequency (LF) less than 200kHz and another is with High Frequency (HF) from 200kHz to 400kHz. A correlation between the density and magnetic fluctuations has been observed. With the n = 2 field applied, an increase of ELM frequency and a drop of electron density (so called density pump-out) have been observed. The electron density (gradient) and pressure (gradient) in the edge pedestal decrease with the application of the n = 2 field while the electron temperature profile shows no change. The experimental observations show that both the density and magnetic fluctuation levels in the edge pedestal are reduced after applying the n = 2 field. This result implies that the ion-scale turbulence in the edge pedestal is not the responsible mechanism for the density pump-out observed during the application of the n = 2 field.

1. INTRODUCTION

The high confinement mode, i.e. H-mode, was first discovered in the ASDEX tokamak [1]. Since then, lots of work has been done to understand the H-mode physics with significant progress being made in experiment [2] and theory [3]. The H-mode is characterized by a spontaneous formation of a transport barrier at the edge pedestal which is usually associated with the repetitive Edge Localized Modes (ELMs). The transport analyses in Refs. [4, 5] have shown that the ion thermal transport coefficient in the edge pedestal region was close to the neoclassical value while the electron thermal transport level was still higher than that predicted by the neoclassical theory. This result suggests that there is remnant turbulence in the pedestal region. In addition, the experimental results on DIII-D [6, 7] and ASDEX Upgrade [8] showed that the pressure gradient in the edge pedestal recovered in a short time after an ELM crash and then saturated for a long time up to the next ELM crash. Electromagnetic turbulence, such as the kinetic ballooning mode [9, 10], has been suggested to be the responsible mechanism for this saturation of the pedestal pressure gradient [7]. These results indicate that the turbulence may play an important role in the pedestal transport process between ELMs.

To gain more fusion power, next step fusion devices, e.g ITER, will be operated primarily in the regime of the ELMy H-mode [11]. Although ELMs provide a natural transport process to control the plasma density and the edge impurity penetration, they also expel a large amount of plasma thermal energy onto the plasma facing components in a few hundred microseconds. The analyses based on an extensive multi-machine ELM database showed the impulsive energy released by the ELM on ITER may reduce significantly the lifetime of the divertor target [12]. This has stimulated the research of ELM control techniques [13]. On DIII-D, the ELM suppression has been realized in the low collisionality H-mode plasmas by applying the Resonant Magnetic Perturbation (RMP) fields with a toroidal mode number (n) of 3 [14]. On JET, n = 1 and n = 2 RMP fields have been used to mitigate the type-I ELMs [15]. A drop of electron density (n_e), i.e. so called density pump-out,

and a reduction of electron pressure (p_e) have been observed during the ELM suppression phase on DIII-D [14] and the ELM mitigation phase on JET [16] while the electron temperature (T_e) shows no reduction. An explanation of the ELM suppression on DIII-D is that the peeling-ballooning (P-B) mode, which is regarded as the most likely candidate to explain the origin of ELMs [17], was stabilised due to the reduction of the pedestal pressure gradient with the application of the n = 3 field [14]. The experimental results from both devices have shown that the reduction of the pressure gradient, mainly due to the density pump-out, during the application of the RMP field was important for the realisations of the ELM suppression or ELM mitigation. A popular explanation of the density pump-out is that the radial particle transport is enhanced due to the stochastisation of the magnetic fields at the edge after applying the RMP field [18, 19, 20, 21]. These analytical or numerical models in Refs. [18, 19, 20, 21] are mainly based on the neoclassical transport theory. The experimental results in L-mode plasmas on TEXTOR have shown that the RMP fields have significant effects on the edge turbulence and turbulence induced transport [22, 23]. Since the L-mode and H-mode plasmas are different, it is important to investigate whether the density pump-out observed in the ELM control experiment is closely related to the turbulence induced transport. If the turbulence is responsible for the density pump-out, it is expected that the turbulence level should increase during the application of the RMP field. In the present work, an X-mode radial Correlation Reflectometry (CR) [24, 25, 26] has been used to study the influence of the RMP field on the turbulence in the edge pedestal on JET.

This paper is organised as follows: after a brief overview of the experimental setup in section 2, the analysis methods are described in section 3. The experimental results are presented in section 4 and a discussion and conclusion are given in section 5.

2. EXPERIMENTAL SETUP

On JET, an n = 2 RMP field, induced by the Error Field Correction Coils (EFCCs) [27], has been applied in the type-I ELMy H-mode plasmas with a toroidal field (B_t) of 2.7T. The EFCCs consist of four planar square shaped coils (~6m in dimension) which are mounted at equally spaced toroidal positions with R = 6m and attached to the transformer limbs. Here, R is the radial distance from the major axis of the machine. Each coil spans a toroidal angle of 70^o and has 16 winding turns. The maximum value of the total current (I_{EFCC}) per coil is 48kAt. The I_{EFCC} is given in terms of the current in one coil winding times the number of turns.

The density fluctuation in the edge pedestal has been measured by using the CR in this experiment. The CR is composed of four independent reflectometry systems [26]. Each system has two channels. One is the xed frequency channel and another is the variable channel with the frequency configurable. The frequencies of the four fixed channels are 76GHz, 85GHz, 92GHz and 103GHz while the frequencies of the four variable channels can be varied in ranges of 76−78GHz, 85−87GHz, 92−96GHz and 100−106GHz. All of the probing waves are directed into the plasma horizontally by using the same antenna (launcher) located at 30.2cm above the equatorial plane

and all of the reflected waves are received by another antenna (receiver), located at 26.8cm above the equatorial plane. Both antennae are installed inside the vacuum vessel at a position of R~4.3m (low field side). Each CR channel is equipped with a quadrature phase detector. More details about the CR can be found in Refs.[24, 25, 26, 28]. Recently, the CR has been used to investigate the characteristics of turbulence on JET [29, 30, 31, 32].

The diagnostic of High Resolution Thomson Scattering (HRTS) [33] has been used to measure n_e and T_e profiles along the outer radius (R = 2.9−3.9m) on the equatorial plane. The repetition rate of the laser pulses determines a sampling rate of 20Hz.

3. ANALYSIS METHODS

Reflectometry is based on a radar technique in which a microwave beam is directed into the plasma with the wave reflected from the cuto layer being detected [34, 35]. Since the phase of the reflected wave is determined by the optical distance, the electron density prole can be derived from the phase variation along the wave path and the density fluctuation can be derived from the phase fluctuation. Due to its simple instruments, the reflectometry has been widely applied to measure density or density fluctuation on present major fusion devices [36, 37]. A quadrature detection allows a complex electrical field ($E = Ae^{i\phi}$) to be reconstructed from the in-phase signal ($I = A\cos\phi$) and quadrature signal ($Q = A\sin\phi$), i.e. $E = I + iQ$, where A is the amplitude and ϕ the phase. In principle, the complex electrical field, amplitude or phase can be used for analysis. In this work, the phase has been used for the analyses of the characteristics of the turbulence in the edge pedestal. The phase jumps are automatically corrected by applying the algorithm introduced in [38].

In the experiment, using radially spaced reflectometry channels, the local wavenumber-frequency spectral density of the phase fluctuation, $S_\phi(k_r, f)$, has been measured by applying the two-point correlation technique [39]. By integrating the frequency components on the measured $S_\phi(k_r; f)$, the radial wavenumber spectral density, $S_\phi(k_r)$ has been calculated, i.e. $S_\phi(k_r) = \sum_f S_\phi(k_r; f)$. The mean wavenumber, $\bar{k}_r$, and the wavenumber spectral width, σ_{k_r}, are defined by

$$\bar{k_r} = \frac{\Sigma_{k_r} k_r S_\phi(k_r)}{\Sigma_{k_r} S_\phi(k_r)}, \qquad \sigma_{k_r} = \sqrt{\frac{\Sigma_{k_r} (k_r - \bar{k_r})^2 S_\phi(k_r)}{\Sigma_{k_r} S_\phi(k_r)}} \tag{1}$$

The radial correlation length of the phase fluctuation, l_r, is defined by the inverse of σ_{k_r}, i.e. $l_r \sqrt{2}/\sigma_{k_r}$ [24].

The measured n_e and T_e gradients in the edge pedestal can be affected by the instrument function of the HRTS [40]. The Full Width at Half Maximum (FWHM) of the HRTS instrument function is between 1cm and 2.5cm, depending on the HRTS hardware configuration and on the plasma equilibrium [41]. In this experiment, the FWHM of the HRTS instrument function is about 1.1cm. To compensate the effect of the instrument function, a forward deconvolution is applied assuming that both the measured and plasma pedestal proles are well described by the modified tanh (MTANH)

function [42]. Two different deconvolution processes are used, one for the ne prole and another for T_e profile. For the n_e, it is assumed that the measured profile is the plasma profile convolved with the HRTS instrument function, while for the T_e, the convolved T_e profile is weigthed with n_e [40].

4. EXPERIMENTAL RESULTS

4.1. CHARACTERISTICS OF TURBULENCE IN THE EDGE PEDESTAL

An example from this experiment is shown in Figure 1 for illustration of the characteristics of the pedestal turbulence. The target plasma is heated by a neutral beam with a total power of 10MW. Figure 1 (a) shows the pedestal density profile, the MTANH fitting curve and the cuto positions of the CR. In this experiment, the fixed channel of the 76GHz reflectometry is not available while the frequency of the variable channel is fixed at 77.7GHz. The frequency spectra of the phase fluctuations measured by the 85GHz and 92GHz reectometries are shown in Figure 1 (b) and the coherence spectrum between the two phase fluctuations is shown in Figure 1 (c). Two broadband fluctuation components have been observed in these spectra. The first one is a Low Frequency (LF) component from f~35kHz to f~200kHz peaked at about 80kHz and another one is a High Frequency (HF) component in the frequency range of 200-400kHz peaked at about 280kHz. The turbulence measurement with Beam Emission Spectroscopy (BES) on DIII-D have shown that the density fluctuation in the edge pedestal also had two broadband fluctuation components, one with lower frequencies (50−150kHz) and another with higher frequencies (200−400kHz) [43]. The frequency spectrum of the magnetic signal ($\delta\dot{B}$) measured by an edge magnetic probe is shown in Figure 1 (b). Here, the magnetic probe is located at 18.4cm above the equatorial plane at R = 3.98m (low field side). In the spectrum of $\delta\dot{B}$, the fluctuation component with the frequency from 35kHz up to 150kHz, showing multi-bands feature, is due to the Washboard (WB) modes [44, 45] while two coherent fluctuations, peaked at f~10kHz and f~30kHz respectively, are due to MHD modes in the plasma core. The WB modes are commonly observed in JET H-mode plasmas and are apparently localised in the pedestal region [45]. They rotate in the Electron Diamagnetic Drift (EDD) direction and usually show multi-bands. The coherence spectrum between the phase fluctuation measured by the 92GHz reflectometry and the magnetic signal is shown in Figure 1 (c). A correlation between the phase fluctuation and the magnetic signal has been observed for the fluctuation component with $f < 150$kHz while no correlation between them is observed for the component with $f > 200$kHz. In addition, this coherence spectrum also shows multi-bands feature from f~35kHz to f~150kHz. The spectrum of $\delta\dot{B}$ shows another fluctuation component peaked at ~320kHz. This component is different from the HF fluctuation registered by the reectometry since they have different peak frequencies and no coherence between them is observed.

4.2. INFLUENCE OF AN N = 2 RMP FIELD ON THE PEDESTAL TURBULENCE

On JET, the influence of an n = 2 RMP field on the pedestal turbulence has been studied. An overview of the ELM mitigation discharge using the n = 2 field is shown in Figure 2. The I_{EFCC}, inducing the

n = 2 field, is applied at 17s, then ramps up to the maximum value of 48kAt in half second and stays at the attop for 2 seconds (about 7 times of the plasma confinement time). With the application of the n = 2 field, the ELM frequency (f_{ELM}) increases from 18Hz to 30Hz and both the core and edge line averaged densities are reduced by about 15%. Figure 3 shows n_e, T_e and p_e profiles before and after the application of the n = 2 field. All the profiles are measured by the HRTS at the last 30% duty cycle of the ELMs. The pe and pe gradient in pedestal are reduced by about 15% after the application of the n = 2 field while the T_e and T_e gradient show no change. The reductions of the p_e and p_e gradient are mainly due to the reductions of the ne and ne gradient in pedestal after applying the n = 2 field.

Figure 4 (a) shows the spectrum of toroidal mode numbers, where the colours denote the toroidal mode numbers n. The n−numbers are obtained by making a time windowed Fourier decomposition of the signals of a toroidal set of edge magnetic probes and analysing the relative phase shift of the fluctuations. After the application of the n = 2 field at 17s, the frequencies of n = 1 and n = 2 core MHD modes decrease. Here, the positive n means that the MHD modes rotate in the Ion Diamagnetic Drift (IDD) direction. This decrease of the core MHD mode frequency is due to the rotation braking with the application of the n = 2 field [15, 46]. However, the frequencies of the WB modes, such as the n = −2WB indicated in Figure 4 (a), have a little increase with the application of the n = 2 field. The mode rotation measured by the magnetic probe is due to the mode rotation in the plasma frame superimposed on the $E_r \times B$ velocity. Here, the $E_r \times B$ velocity is due to the plasma radial electrical field (E_r). It is not known why the frequencies of the WB modes increase after applying the n = 2 field since there is no accurate measurement of the E_r in the edge pedestal region at the moment. Figure 4 (b) shows the power spectra of the magnetic signals. What we are interested in are the fluctuation component with the frequency from 30kHz to 200kHz, i.e. the WB modes. It can be seen from the figure that the power of this component decreases with the application of the n = 2 field. Further, the time evolution of the magnetic fluctuation level (δB) is shown in Figure 2 (e). Here, the δB is calculated for the fluctuation component with the frequency from 35kHz to 200kHz, avoiding the core MHD modes, from the $\delta\dot{B}$ measured by the edge magnetic probe. Only the data measured at the last 30% duty cycle of ELMs are used. This result shows that the values of δB during the flattop of the I_{EFCC} are only about 30% of those before the application of the n = 2 field. During the application of the EFCCs induced field on JET, the feedback response to the field in the magnetic control sensors either shrinks or expands the plasma column, depending on the EFCC phase [33]. The examples of the two cases are the Pulse No's: 69557 (shrinking) and 69558 (expanding), as shown in the Figure 6 and Figure 10 respectively in Refs.[33]. In the present experiment, the plasma column is shrank with the application of the n = 2 field. This means that the distance between the locations of the pedestal and the magnetic probe increases after applying the n = 2 field. The analysis for Pulse No's: 69557 and 69558 show that the magnetic fluctuation levels decrease during the ELM mitigation phase in both pulses although one is with the plasma shrinking and another with the plasma expanding. This indicates that the reduction of the magnetic

fluctuation level observed in the present experiment is not due to the increase of the distance between the pedestal plasma and the magnetic probe.

Figure 5 (b) shows the coherence spectra between the phase fluctuations measured by two radially spaced CR channels, i.e. the 77.7GHz and 85GHz reflectometry. The cuto position of the 77.7GHz reflectometry is at about $\psi_N = 0.977$ and doesn't change with the application of the n = 2 field while the cuto position of the 85GHz reectometry moves a little bit inside, from $\psi_N = 0.97$ to $\psi_N = 0.967$. After the application of the n = 2 field, the peak frequency of the LF fluctuation decreases from 100kHz to 50kHz while the peak frequency of the HF fluctuation increases from about 250kHz to 280kHz. This result implies that the LF and HF fluctuations rotate in opposite directions in the plasma frame although we don't know the exact direction (IDD or EDD) for each fluctuation based on present data. The two broadband density fluctuations in pedestal observed on DIII-D also rotate in opposite directions in the plasma frame: the lower frequency band (50-150kHz) is in the IDD direction while the higher frequency band (200-400kHz) is in the EDD direction [43]. Figure 5 (b) further shows that the coherence values at all the frequencies of the HF fluctuation increase after the application of the n = 2 field while the coherence value at the peak frequency of the LF fluctuation also increases. Figure 5 (a) shows that the phase fluctuation level of LF fluctuation decreases with the application of the n = 2 field. The integrated power of the HF fluctuation also decreases after applying the n = 2 field although the power at f~280 kHz has an increase, which is due to the upshift of the frequencies of the HF fluctuation. The decreases of the LF and HF phase fluctuation levels are more evident in Figure 2 (f) and (g) which show the time evolutions of the LF and the HF phase fluctuation levels (σ_ϕ) respectively. These σ_ϕ are calculated from the phase fluctuations measured by the 77.7GHz reflectometry. In this calculation, the frequency changes of the LF and HF fluctuations with the application of the n = 2 field have been taken into account. For the LF fluctuation, the values of decrease from about 1.2 rad to 0.8 rad (Figure 2 (f)) with the application of the n = 2 field and the of the HF fluctuation also shows a decrease, from about 0.3 rad to 0.25 rad (Figure 2 (g)). Figure 5 (c) and (d) show the radial wavenumber spectral density of the phase fluctuation, $S_\phi(k_r)$, in the edge pedestal. The $S_\phi(k_r)$ is calculated from the phase fluctuations measured by the 77.7GHz reflectometry and the 85GHz reflectometry, by applying the method introduced in section 3. The wavenumber spectral width (σ_{k_r}) of the LF fluctuation decreases from ~2.0cm^{-1} to 6 1:2cm^{-1} and thus the radial correlation length of the phase fluctuation (l_r) increases from ~0.71cm to ~1.17cm with the application of the n = 2 field. For the HF fluctuation, the σ_{k_r} decreases from ~3cm^{-1} to ~ 1.55cm^{-1} and thus the l_r increases from ~0.47cm to ~0.9cm after applying the n = 2 field. Many analytical theories and simulations of the reflectometry, such as those in Ref.[34, 35, 49, 50, 51, 52, 53, 48], have shown that quantities analysed from the reflectometry data have complex relations with the plasma turbulence quantities. To interpret the reflectometry data, several two-dimensional (2D) full-wave simulations have been utilized in the community. One of them is introduced in [47, 48]. In this 2D simulation, the coherent reflection G [48] and the radial correlation length analysed from the reflectometry data are needed to map the turbulence quantities, i.e. the turbulence level

and radial correlation length. One example of such mapping has been shown in Fig.3 in Ref.[48]. Here, the G is defined by $G = |<E>|/\sqrt{<|E|^2>}$ [48], where <> denotes ensemble average and E is the complex reected wave field. Presently, we use a simplified analytical expression to estimate the G, i.e. $G = e^{-\sigma_\phi^2/2}$, which is derived from the phase screen model [49, 50] or [52]. For the LF fluctuation, the G increases from 0.48 (with $\sigma_\phi = 1.2$) to 0.73 (with $\sigma_\phi = 0.8$) with the application of the n = 2 field while for the HF fluctuation, the G increases from 0.956 (with $\sigma_\phi = 0.3$) to 0.97 (with $\sigma_\phi = 0.25$). Since both G and l_r increases with the application the n = 2 field, i.e. the point moving from bottom left to top right in Fig.3 in Ref.[48], the density fluctuation levels of the LF and HF fluctuations should decrease. The reduction of the edge turbulence with the application of the RMP fields has been observed in L-mode plasmas on TEXTOR [22, 23].

DISCUSSION AND CONCLUSION

The CR on JET is predominantly sensitive to the fluctuation with a wave number ($k_\perp$) less than $1.2cm^{-1}$ [29] or $k_\perp\rho_i < 0.36$ (calculated using $T_i = 1.5keV$), i.e, the ion-scale turbulence [54]. Here, ρ_i is the ion gyro-radius. During the application of the n = 2 field, the density pump-out, i.e. enhancement of particle transport, has been observed. If the turbulence in the pedestal measured by the reflectometry is responsible for the density pump-out, it is expected that the amplitude of this turbulence should increase with the application of the n = 2 field. However, the analysis in section 4 have shown that both the long wavelength magnetic fluctuation, mainly the WB modes measured by the magnetic probe, and the ion-scale density fluctuation measured by the CR in the edge pedestal decrease after applying the n = 2 field. This result implies that the observed density pump-out is not directly related to the WB modes and the ion-scale density fluctuations in the pedestal on JET. The influence of an n = 3 RMP field on the turbulence has been studied on DIII-D [55, 56]. Their results showed that the ion-scale density fluctuation ($k_\perp\rho_i < 0:3$) measured by BES in the pedestal didn't change when the ELMs were suppressed by applying the n = 3 field, while a significant increase of the ion-scale turbulence level was observed in the plasma core region [55, 56]. On the other hand, the intermediate scale turbulence ($k_\perp \sim 4.2cm^{-1}$ or $k_\perp\rho_i \sim 0.8$) in the pedestal measured by the Doppler backscatter reflectometry often showed an increase after the ELM suppression with the n = 3 field [56]. These results imply that the ionscale turbulence in the core and the intermediate scale turbulence in the pedestal may be important for the enhancement of the particle transport during the ELM suppression phase on DIII-D. Presently, the reflectometry measurement on JET can not give a definite answer about how the ion-scale turbulence in the plasma core changes after the ELM mitigation since the cuto positions of the CR in the core are very different before and during the application of the RMP field. Nevertheless, both results on JET and DIII-D [55, 56] show that the ion-scale turbulence in pedestal is not the responsible mechanism for the density pump-out observed during the application of the RMP fields. The fact that the T_e and T_e gradient are not changed while the turbulence is reduced with the application of the n = 2 field suggests that the observed magnetic and density fluctuation in the edge pedestal on JET are not driven by the T_e gradient. The reduction

of the pedestal turbulence may be due to the reduction of the density or pressure gradients.

In conclusion, the experimental observations on JET have shown that the ion-scale turbulence in the edge pedestal can be reduced by using an n = 2 RMP field in the type-I ELMy H-mode plasmas. This result implies that the ion-scale turbulence in the edge pedestal is not the responsible mechanism for the enhancement of the particle transport (density pump-out) observed during the application of the n = 2 field on JET.

ACKNOWLEDGEMENTS

The authors would like to thank A Krämer-Flecken and M Z Tokar for useful discussions. This work, supported by the European Communities under the contract of Association between EURATOM and FZJ, was carried out within the framework of the European Fusion Development Agreement. Additional support from the Helmholtz Association in frame of the Helmholtz-University Young Investigators Group VH-NG-410 is gratefully acknowledged. The views and opinions expressed herein do not necessarily reect those of the European Commission.

REFERENCES

[1]. Wagner F. et al 1982 Physical Review Letters **49** 1408-12
[2]. Wagner F. 2007 Plasma Physics and Controlled Fusion **49** B1-33
[3]. Connor J.W. and Wilson H R 2000 Plasma Physics and Controlled Fusion **42** R1-74
[4]. Stacey W.M. 2004 Physics of Plasmas **11** 1511-19
[5]. Callen J.D. et al 2010 Nuclear Fusion **50** 064004
[6]. Groebner R.J. et al 2009 Nuclear Fusion **49** 045013
[7]. Groebner R.J. et al 2010 Nuclear Fusion **50** 064002
[8]. Burckhart A. et al 2010 Plasma Physics and Controlled Fusion **52** 105010
[9]. Snyder P.B. et al 2009 Physics of Plasmas **16** 056118
[10]. Yan Z. et al 2011 Physical Review Letters **107** 055004
[11]. ITER Physics Basis Editors et al 1999 Nucl. Fusion **39** 2175
[12]. Loarte A. et al 2003 Journal of Nuclear Materials **313-316** 962-66
[13]. Doyle E.J. et al 2007 Nuclear Fusion **47** S18-S127
[14]. Evans T. et al 2006 Nature of Physics **2** 419
[15]. Liang Y. et al 2010 Nuclear Fusion **50** 025013
[16]. Liang Y. et al 2007 Physical Review Letters **98** 265004
[17]. Snyder P.B. et al 2004 Plasma Physics and Controlled Fusion **46** A131
[18]. Tokar M.Z. et al 2007 Physical Review Letters **98** 095001
[19]. Tokar M.Z. et al 2008 Plasma Physics and Controlled Fusion **48** 024006
[20]. Park G. et al 2010 Physics of Plasmas **17** 102503
[21]. Rozhansky V. et al 2010 Nuclear Fusion **50** 034005
[22]. Xu Y. et al 2006 Physical Review Letters **97** 165003
[23]. Xu Y. et al 2009 Nuclear Fusion **49** 035005

[24]. Conway G.D. et al 1999 Review of Scientific Instruments **70** 3921-29
[25]. Hacquin S. et al 2004 Review of Scientific Instruments **75** 3834-36
[26]. Hacquin S. et al 2006 Review of Scientific Instruments **77** 10E925
[27]. Barlow I. et al 2001 Fusion Engineering and Design **58-59** 189
[28]. Cupido L. et al 2005 Fusion Engineering and Design **74** 707-713
[29]. Conway G.D. et al 2000 Physical Review Letters **84** 1463.
[30]. Conway G.D. et al 2002 Plasma Physics and Controlled Fusion **44** 1167.
[31]. Figueiredo A.C.A, et al. 2008 Review of Scientific Instruments **79** 10F107
[32]. Figueiredo A.C.A, et al. 2009 36th EPS Conference on Plasma Phys. Soa, 2009 ECA Vol.33E, P-2.167
[33]. Aler A. et al 2008 Nuclear Fusion **48** 115006
[34]. Mazzucato E. 1998 Review of Scientific Instruments **69** 2201-16
[35]. Nazikian R. et al 2001 Physics of Plasmas **8** 1840-55
[36]. Laviron C. et al 1996 Plasma Physics and Controlled Fusion **38** 905-36
[37]. Conway G.D. 2006 Nuclear Fusion **46** S665-69
[38]. Ejiri A. et al 1997 Plasma Physics and Controlled Fusion **39** 1963-80
[39]. Beall J.M. et al 1982 Journal of Applied Physics **53** 3933
[40]. Scannel R. et al 2011 Review of Scientific Instruments **82** 053501
[41]. Frassinetti L. et al, to be submitted to Review of Scientific Instruments
[42]. Groebner R.J. et al 2001 Nuclear Fusion **41** 1789-1802
[43]. Yan Z. et al 2011 Physics of Plasmas **18** 056117
[44]. Smeulders P. et al 1999 Plasma Physics and Controlled Fusion **41** 1303.
[45]. Perez C.P. et al 2004 Plasma Physics and Controlled Fusion **46** 61-87
[46]. Sun Y. et al 2010 Plasma Physics and Controlled Fusion **52** 105007.
[47]. Valeo E.J. et al 2002 Plasma Physics and Controlled Fusion **44** L1-L10.
[48]. Kramer G.J. et al 2003 Review of Scientific Instruments **74** 1421-25
[49]. Mazzucato E. and Nazikian R. 1993 Physical Review Letters **71** 1840
[50]. Nazikian R. and Mazuccato E. 1995 Review of Scientific Instruments **66** 392-398
[51]. Conway G.D. 1997 Plasma Physics and Controlled Fusion **39** 407-21
[52]. Gusakov E.Z. and Popov A Yu 2002 Plasma Physics and Controlled Fusion **44** 2327-37
[53]. Gusakov E.Z. et al 2002 Plasma Physics and Controlled Fusion **44** 1565
[54]. Horton W. 1999 Review of Modified Physics **71** 735.
[55]. Yan Z. et al 2010 The 23rd IAEA Fusion Energy Conference 2010, Daejon, Korea. http: //www-pub.iaea.org/mtcd/meetings/PDFplus/2010/cn180/cn180_papers/exc_p3-05.pdf
[56]. Moyer R A et al 2011 'Impact of Resonant Magnetic Perturbations on Turbulence Drives, Damping, and Transport' The 5th International Workshop on Stochasticity in Fusion Plasma, Juelich, Germany 2011.

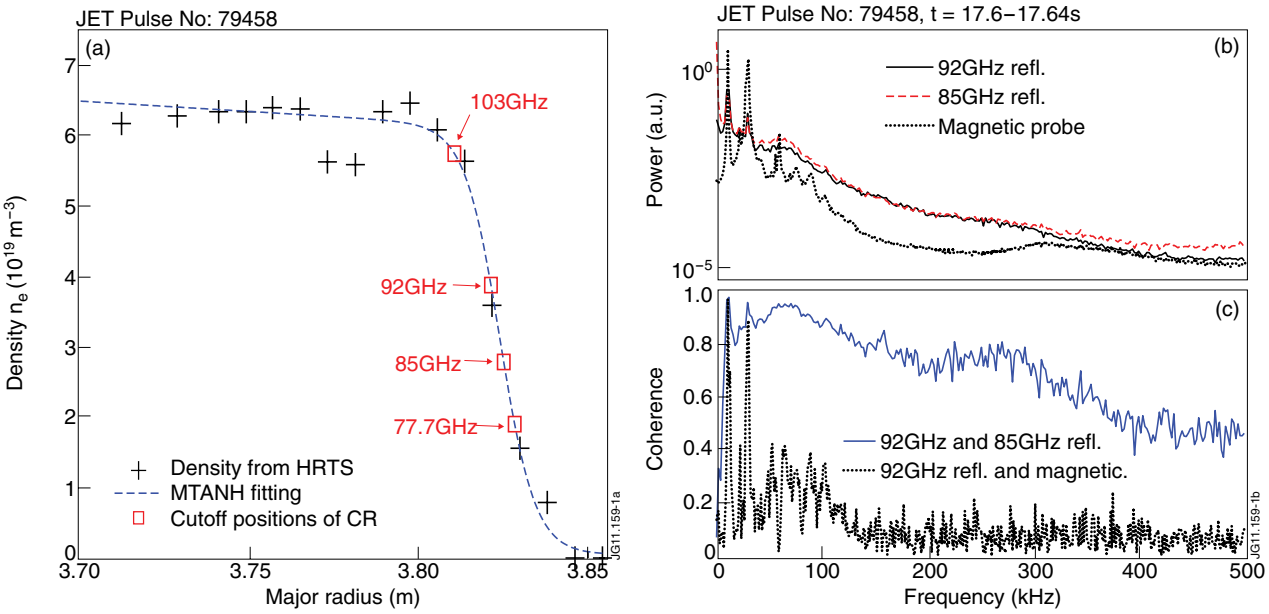

Figure 1: (a) The edge density profile and the cuto positions of the CR. (b) The frequency spectra of ϕ measured by the CR and the spectrum of $\delta\dot{B}$ measured by the edge magnetic probe. (c) The coherence spectrum between the ϕ (thin line) measured by two radially spaced CR channels and the coherence spectrum between the and $\delta\dot{B}$ (thick line).

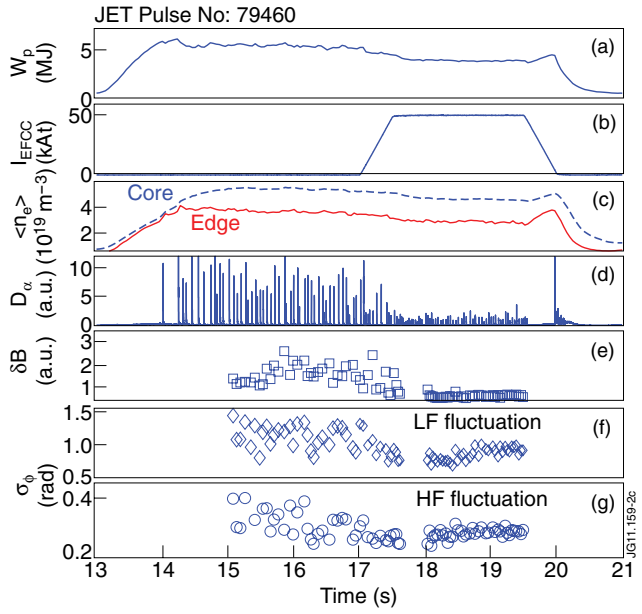

Figure 2: An overview of an ELM mitigation discharge using an n = 2 RMP field: (a) plasma energy, W_P (b) the applied EFCC current, I_{EFCC} (c) core (dash line) and edge (solid line) line averaged density (d) D_α lines from inner divertor (e) the magnetic fluctuation level, δB in the frequency range of 35kHz< f <200kHz (f) and (g) the phase fluctuation level (σ_ϕ) of the LF turbulence and the HF turbulence measured by the 77.7GHz reflectometry.

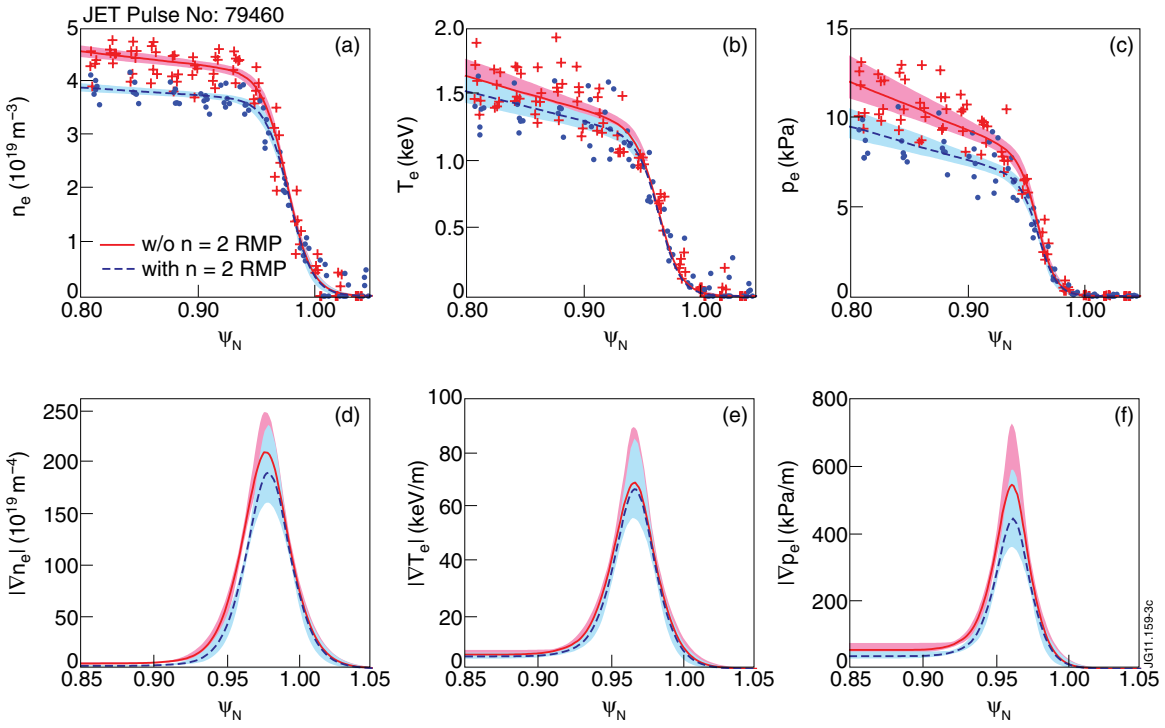

Figure 3: The n_e, T_e and P_e profiles (top) in the last 30% duty cycle of ELMs and correspondent gradients (bottom), without and with the n = 2 RMP field (solid and dash line, respectively). The lines show the deconvolved fits and the shaded areas the corresponding uncertainties.

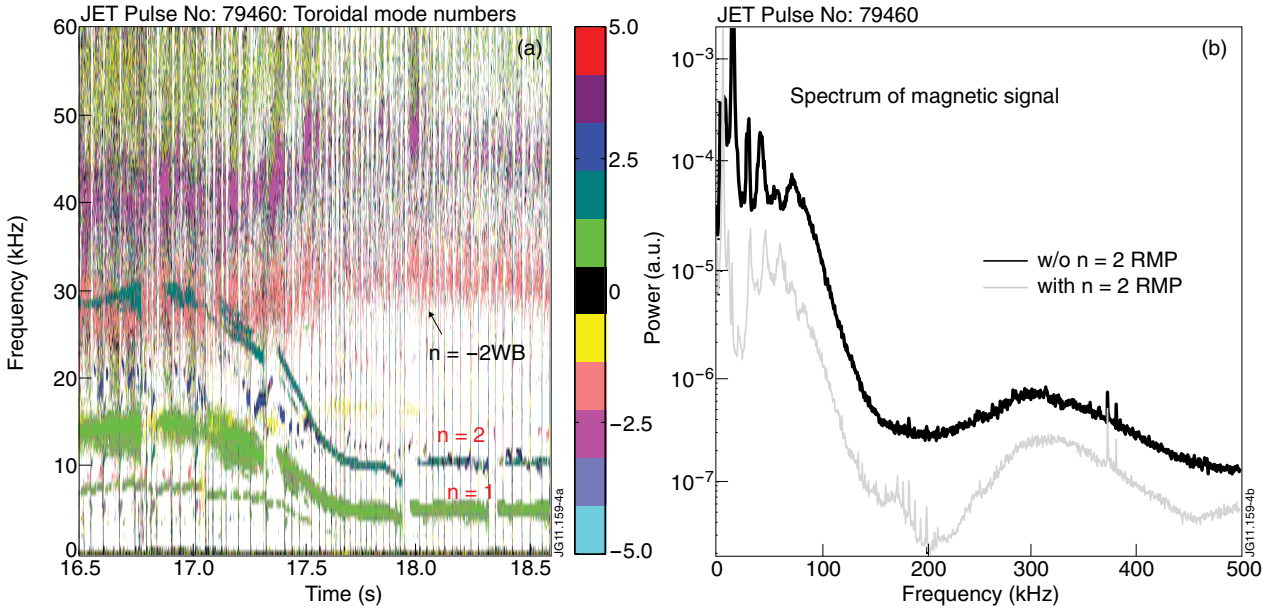

Figure 4: (a) Spectrum of the toroidal mode number (b) Comparison of the spectra of the magnetic signal before and after the application of the n = 2 field.

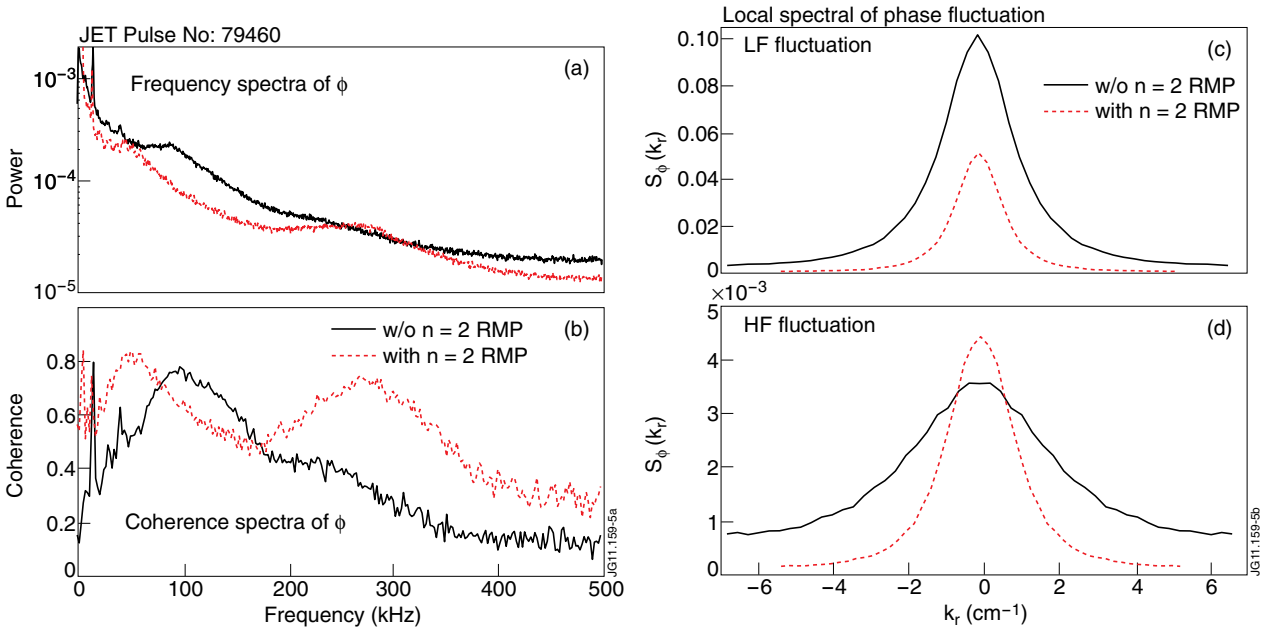

Figure 5: (a) The spectra of the phase fluctuations measured by the 77.7GHz reflectometry (b) The coherence spectra between the phase fluctuations measured by the 77.7GHz and 85GHz refelctometry (c) The radial wavenumber spectral density of the phase fluctuations, $S_\phi(k_r)$, for LF fluctuation and (d) the $S_\phi(k_r)$ for HF fluctuation.